Organic & Biomolecular Chemistry

COMMUNICATION

Cite this: *Org. Biomol. Chem.*, 2019, **17**, 7878

Received 28th June 2019,
Accepted 5th August 2019

DOI: 10.1039/c9ob01459d

rsc.li/obc

Dendritic architectures by orthogonal thiol-maleimide "click" and furan-maleimide dynamic covalent chemistries†

Stephen H. Frayne, Robert M. Stolz and Brian H. Northrop *

A set of dendrons and dendrimers is synthesized divergently using an orthogonal combination of kinetically-driven thiol-maleimide "click" chemistry and thermodynamically reversible furan-maleimide cycloaddition/retrocycloaddition reactions. Growth is controlled by taking advantage of the selective thiol–ene addition of thiols to the electron withdrawn alkene of maleimide in the presence of electron rich alkene of oxanorbornene. Subsequent activation of growing dendrons/dendrimers requires only heat to induce the dynamic covalent liberation of peripheral furan protecting groups. The methodology introduced provides a new route to multifunctional dendrimers that could, in principle, be synthesized by introducing different branched monomers at any stage of dendrimer growth, allowing dendrimer architectures and properties to be better tailored to their intended applications.

Introduction

For the past few decades dendrimers,[1–4] highly branched globular macromolecules, have found applications spanning multiple areas of catalysis,[5–7] medicine,[8–10] and materials science.[11–14] Dendrimers offer considerable promise and advantages relative to more traditional macromolecules given their monodispersity and well-defined chemical architectures. Despite their promise, however, synthetic hurdles often hamper the development of dendrimer chemistry. In particular, most protocols for the synthesis of dendrimers remain tedious and require laborious purification because of unreacted starting materials, side products, and structural defects that result from incomplete conversion during growth and/or activation steps. The emergence of click chemistry[15–18] in 2001 brought a new classification of reactions that are "spring loaded" to afford selective, efficient, atom economical, and high yielding synthetic transformations. These desirable attributes make click reactions particularly well suited to the challenges of dendrimer synthesis,[19] especially when following divergent protocols where the number of reactions necessary for defect-free dendrimers increases exponentially with each successive growth step. It is therefore unsurprising that several research groups[20–30] have made great use of click reactions in the divergent synthesis of a variety of dendrimers. In 2008, for example, Hawker used photo-initiated thiol–ene click chemistry paired with efficient esterification reactions for the facile synthesis of fourth generation dendrimers that could be readily functionalized using additional thiol–ene reactions.[21] Shortly thereafter the Hawker group demonstrated that the combination of two different, orthogonal click protocols – thiol–ene click and copper-catalyzed alkyne–azide cycloadditions (CuAAC) – could be utilized to prepare a sixth generation dendrimer using only growth steps,[23] therefore significantly streamlining dendrimer synthesis by forgoing the need for activation steps altogether. The Bowman group has reported that even a single class of click reactions, when appropriately designed, can be used to synthesize fifth generation dendrimers rapidly and efficiently.[26] Their success rested on the use of kinetically selective thiol-Michael reactions, again without requiring any protection/deprotection steps.

These examples highlight several of the advantages of using orthogonal click reactions in the divergent synthesis of dendrimers, however they also reveal a potential limitation of the approach: dendrimers synthesized using two orthogonal or selective protocols will produce layered dendrimers of a single specific sequence. That is, a trade off of avoiding protection/deprotection steps is the fact that growth steps can only occur by sequentially alternating the order of branched monomers used, resulting in dendrimers with alternating layers A-B-A-B-A- *etc.*, where "A" and "B" are two different types of branched monomers possessing the requisite orthogonal reactive groups (Scheme 1A). It is less straightforward to use this approach to prepare dendrimers containing any desired sequence of

Wesleyan University, Department of Chemistry, 52 Lawn Ave., Middletown, CT 06459, USA. E-mail: bnorthrop@wesleyan.edu; Fax: +1 860 685-2211; Tel: +1 860 685-3987

† Electronic supplementary information (ESI) available: Materials and methods, full synthetic procedures, NMR and mass spectra. See DOI: 10.1039/c9ob01459d

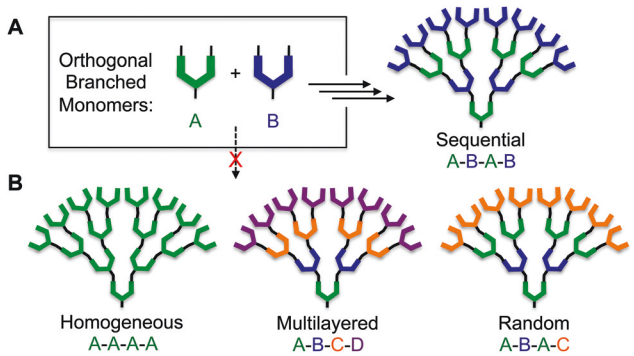

Scheme 1 The use of two branched monomers that exhibit orthogonal reactivity allows rapid access to sequentially branched dendrimers (A), however orthogonality can inhibit access to homogeneous, multilayered, and random dendrimers (B).

branched monomers, *e.g.* homogeneous (A-A-A-A-...), multilayered (A-B-C-D-...), random (A-B-A-C-...), *etc*. Recently, Roy and coworkers[27,28,30] have used orthogonal combinations of thiol–ene, thiol–yne, esterification, CuAAC, and/or S_N2 reactions to synthesize multilayered and heterolayered glycodendrimers. Still, to the best of our knowledge, there are not yet protocols that enable a straightforward "mix and match" approach to the preparation of all types of dendritic architectures shown in Scheme 1.

Herein we report a proof-of-concept design wherein the orthogonality of efficient thiol-maleimide click reactions[31] and dynamic covalent furan-maleimide cycloaddition reactions[32] can be used to synthesize a variety of differently layered dendritic architectures from only a small collection of branched monomer building blocks. The design begins with the synthesis of monomers bearing a thiol focal point and furan-protected maleimide branches, such as compounds **1** and **2** shown in Fig. 1. Any such monomers can be combined in any order as represented in Scheme 1B by taking advantage of the efficient reaction of thiols with maleimide (growth steps) followed by the efficient removal of peripheral furan protecting groups by simply heating at reduced pressure (activation steps). This methodology affords complete control over the resulting dendritic architecture and enables dendrimer properties, such as hydrophilicity/hydrophobicity, cavity size, and branching to be tailored specifically to match the intended application of the dendrimer by incorporating any chosen branched monomer at any stage of dendrimer growth. In this communication we report an initial proof-of-concept of this design by synthesizing three different dendrons or dendrimers from the two new branched monomers **1** and **2**.

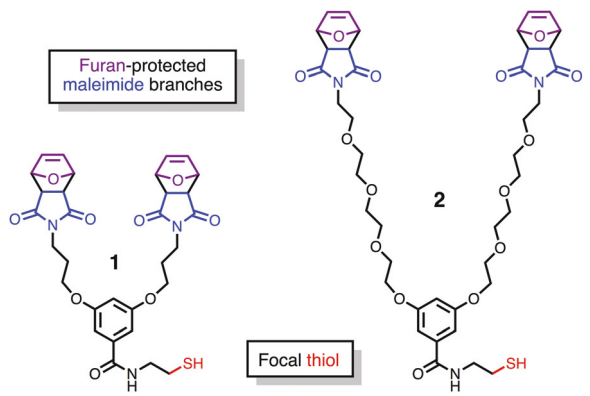

Fig. 1 Chemical structures of branched monomers **1** and **2**.

Results and discussion

The syntheses of monomers **1** and **2** are outlined in Schemes S2 and S3 of the ESI.† Both monomers are built upon a 3,5-dihydroxybenzoic acid core. Where they differ is in the choice of linker joining the aryl core to peripheral furan-protected maleimide functionalities. Monomer **1** has a shorter, more hydrophobic propyl linker while monomer **2** has a longer, more hydrophilic tetraethylene glycol linker. Both monomers have a focal benzyl amide thiol functionality, which was chosen for its stability under aerobic oxidative conditions. It is the focal thiol and peripheral furan-protected maleimide design of monomers **1** and **2** that underlies the basis of the approach reported herein. One drawback of the specific AB_2 monomers shown in Fig. 1 is that each requires several synthetic steps to prepare, somewhat undercutting the goal of increasing overall synthetic efficiency. Fortunately, procedures for **1** and **2** have been optimized to allow most intermediates to be purified by recrystallization such that target monomers can be prepared on the gram scale, and more efficient routes to similarly designed AB_2 monomers are being explored.

To test the design protocol reported herein, monomer **1** was first used to synthesize homogeneous, fourth generation dendron **3** (Fig. 2E) and third generation dendrimer **4**. Dendron **3** was built from an *N*-methylmaleimide (NMM) core while the synthesis of dendrimer **4** was built upon a tris-maleimide core (tris-M) that is readily synthesized from mesitylene.[33] Spectroscopic signals that are diagnostic for maleimide and the furan-maleimide adduct are especially useful for following the growth and activation steps during the synthesis of compounds **3** and **4**. A representative example is shown in Fig. 2. A partial ^{1}H NMR spectrum of the mixture of NMM and monomer **1** prior to their thiol-maleimide reaction is shown in Fig. 2A. Singlets corresponding to the vinylic protons of NMM (H^a, blue) and the allylic and vinylic protons of the pendant furan adduct of **1** (H^g and H^h, purple) appear at 6.7, 6.5, and 5.3 ppm, respectively. The addition of catalytic triethylamine (TEA) promotes the selective addition of the thiol of **1** to the electron withdrawn vinyl group of NMM (growth step), leaving the electron rich vinylic group of the furan adduct untouched.[34] This selectivity is indicated by the disappearance of the maleimide singlet at 6.7 ppm, retention of both furan signals at 6.5 and 5.3 ppm, and the appearance of a methine doublet of doublets corresponding to H^i at 3.7 ppm (Fig. 2B). The resulting compound is labeled $G1_F$ to indicate that it is a first generation dendron that is furan-protected.

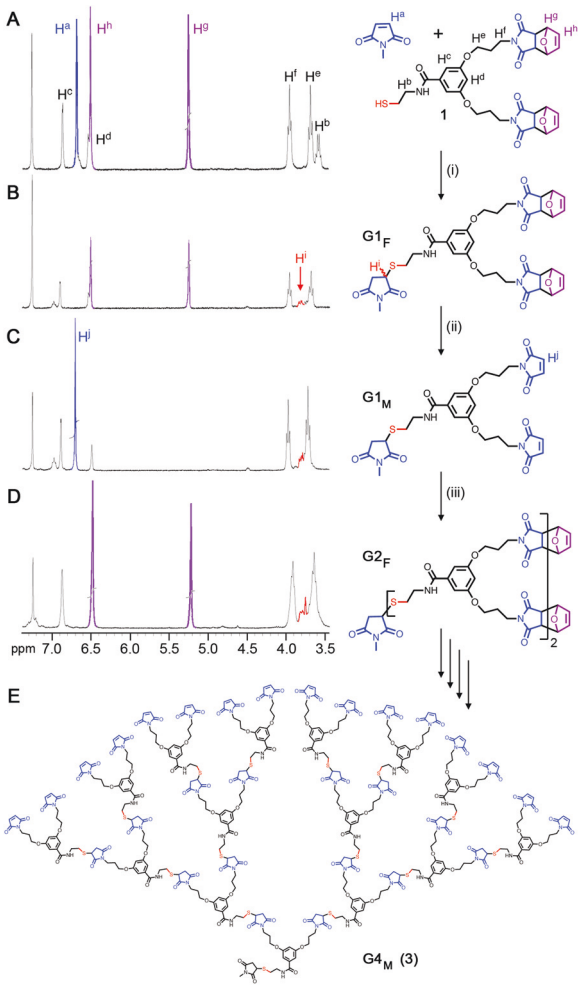

Fig. 2 Partial ^{1}H NMR spectra of a mixture of **1** and NMM (A), $G1_F$ (B), $G1_M$ (C), and $G2_F$ (D) as well as the chemical structure of $G4_M$ (E). Reagents and conditions: (i) TEA, $CHCl_3$; (ii) anisole, 140 °C, 1 h; (iii) **1**, TEA, $CHCl_3$.

The subsequent deprotection of $G1_F$ can be achieved by heating the protected compound to 140 °C in anisole for 1 hour,[35] which induces a retro-Diels–Alder reaction to give $G1_M$, *i.e.* a first generation dendron that bears peripheral maleimide functionalities (Fig. 2C). Again, structural characteristics inherent in the molecular design enable straightforward monitoring of the reaction progress. Thermal deprotection of $G1_F$ results in the disappearance of allylic and vinylic signals at 6.5 and 5.3 ppm concomitant with the re-appearance of a maleimide singlet (H^j) at 6.7 ppm. An advantage of using furan as a protecting group is that it's low boiling point helps drive the dynamic covalent retrocyclization toward the product while its evaporation also serves to purify the desired compound. Removal of anisole is achieved by passing the $G1_M$ solution over a short pad of silica and eluting with hexanes. The maleimide-functionalized growing dendron can then be eluted using a mixture of dichloromethane and methanol. In this case passing the product over silica is not a prerequisite for obtaining a pure product, rather it is simply used as a means of removing anisole. Reaction of the deprotected $G1_M$ dendron with 2 equivalents of branched monomer **1** in $CHCl_3$ and catalytic TEA results in a second growth step to produce $G2_F$, as shown in Fig. 2D. The disappearance of the maleimide singlet H^j (6.7 ppm) and reappearance of allylic and vinylic signals (6.5 and 5.3 ppm, respectively) provide clear support for successful dendron growth.

This process of thiol-maleimide click growth steps followed by thermally promoted retro-Diels–Alder activation steps – *i.e.* "click-heat-click-heat" – was repeated to provide 4th generation dendron $G4_M$ (**3**, Fig. 2E). ^{1}H and ^{13}C NMR spectroscopy support the formation of monodisperse dendron products (see spectra in section IV of the ESI†). GPC and mass spectrometric analysis also provide evidence of complete conversion during growth and activation steps. GPC traces were acquired for dendrons $G1_F$ through $G3_M$ in THF and are shown in Fig. 3A. For each generation there is a clear distinction between furan-protected dendrons (GX_F) and maleimide-functionalized dendrons (GX_M). Steric bulk of the oxanorbornene moiety of furan-protected dendrons relative to planar maleimide moiety of activated dendrons causes the GX_F compounds to elute earlier than their GX_M analogues. The difference between the apogees of the GPC traces within the same generation (*e.g.* $G1_F$ *vs.* $G1_M$) roughly doubles with each generational increase. This is consistent with the fact that the number of furan molecules lost during each retro-Diels–Alder activation step doubles during exponential growth of the dendron. Polydispersity indices (PDI) for the series all fall between 1.02–1.09, consist-

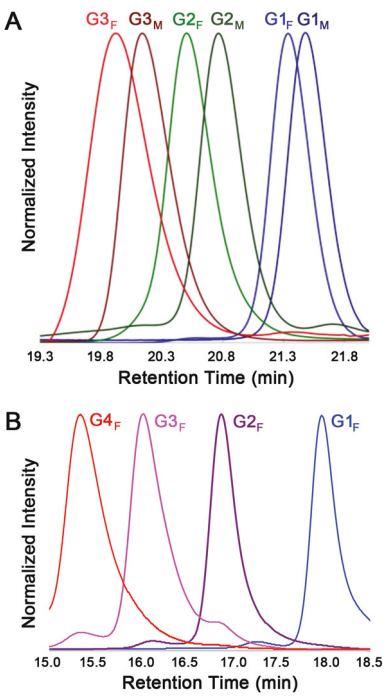

Fig. 3 GPC traces of furan-protected and maleimide-functionalized dendrons up through G3 recorded with THF as the eluent (A) and GPC traces of G1-G4 furan-protected dendrons obtained with DMF as the eluent on account of the poor THF solubility of G4 dendrons (B).

Table 1 Characterization of dendrons $G1_F$ through $G4_M$ by mass spectrometry and GPC

Dendron	M_{calc}	M_{obs}	M_n	PDI
$G1_F$	735.23	735.24[a]	647[d]	1.02
$G1_M$	599.18	599.18[a]	548[d]	1.03
$G2_F$	1845.57	1845.57[a]	1534[d]	1.05
$G2_M$	1573.46	1573.46[a]	1185[d]	1.03
$G3_F$	4088.22	—[b]	2737[d]	1.06
$G3_M$	3544.01	3546.0[c]	2186[d]	1.04
$G4_F$	8529.56	—[b]	2533[e]	1.09
$G4_M$	7441.14	7443.5[c]	—[f]	—[f]

[a] ESI-TOF $[M + H]^+$ results. [b] No furan-protected parent ion peak observed. [c] MALDI-TOF $[M + Na]^+$ results. [d] Calibrated by poly(methyl methacrylate) standards. [e] Calibrated by polystyrene standards. [f] GPC analysis was unsuccessful due to insufficient dendron solubility.

ent with the formation of monodisperse dendrons (Table 1). Beginning with the 4th generation ($G4_F$) the dendrons were no longer soluble in THF and therefore Fig. 3B shows GPC traces of all four furan-protected dendrons $G1_F$ through $G4_F$, which were obtained with DMF as the eluting solvent. PDI values for $G1_F$–$G4_F$ in DMF range from 1.03–1.09, again indicating monodisperse dendrons though small shoulders can be observed in the DMF results, particularly in the case of $G3_F$. This may suggest small amounts of incomplete conversion, though it is worth noting that similar shoulders are essentially absent from results in THF and evidence of incomplete conversion was not observed in ^{1}H NMR spectroscopic results.

Characterization by mass spectrometry was carried out using ESI-TOF MS for dendrons up through generation two and by MALDI-TOF MS to characterize generations three and four (Table 1). ESI $[M + H]^+$ signals for dendrons $G1_F$ through $G2_M$ agree very well with their calculated masses. Higher mass dendrons ≥G3 were investigated by MALDI, however a parent $[M + Na]^+$ ion was only observed for the maleimide-functionalized dendrons $G3_M$ and $G4_M$. Furan-protected dendrons $G3_F$ and $G4_F$ did not show parent ion peaks. Interestingly, MALDI-TOF spectra of $G3_F$ and $G4_F$ did positively identify the $[M + Na]^+$ ion of their deprotected analogues $G3_M$ and $G4_M$, respectively (see Fig. S45 and S47 of the ESI†). It is possible that the rapid heating under vacuum during MALDI analysis results in loss of peripheral furan moieties from $G3_F$ and $G4_F$, and therefore only their deprotected parent ions are observed.

The same "click-heat" process was then used to synthesize 3rd generation dendrimer **4**, as shown graphically in Scheme 2. As before, diagnostic ^{1}H NMR spectroscopic signals provide a clear and convenient means of quickly evaluating the growth and activation steps based on the same diagnostic signals highlighted in Fig. 2. MALDI-TOF MS again suggests that ionization conditions promote the loss of peripheral furan moieties. For example, the MALDI signal for the $G1_F$ dendrimer was observed at *m*/*z* of 1889.7, which corresponds well with the calculated $[M + Na]^+$ of 1889.5 for $G1_M$ (see Fig. S50 of the ESI†). Approximately the same mass (*m*/*z* of 1890.9) was, unsurprisingly, observed upon analysis of the $G1_M$ dendrimer itself. Similar results were observed up through $G3_F$ dendrimer

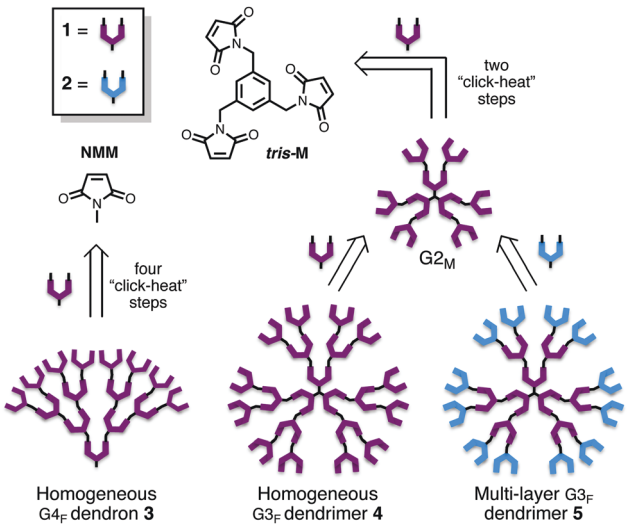

Scheme 2 Summarized representation of the synthetic routes to homogeneous $G4_F$ dendron (**3**) from **NMM** as well as homogeneous $G3_F$ dendrimer (**4**) and multi-layered $G3_F$ dendrimer (**5**) from **tris-M**.

4, for which an $[M + Na]^+$ signal of 10 662.4 was found that closely matches the mass of 10 658.1 calculated for $G3_M$ (Fig. S60 of the ESI†). These observations lend further support to the hypothesis that MALDI analysis promotes loss of furan through a retro-Diels–Alder reaction. Unfortunately the solubility of the growing dendrimer decreased significantly with each generation, preventing growth beyond generation 3 and complicating GPC analysis for dendrimers above $G2_M$. Fig. 4 shows GPC traces for dendrimers $G1_F$ through $G2_M$ that were sufficiently soluble to allow analysis in DMF. Dendrimers $G1_F$ to $G2_M$ were not as monodisperse as the dendrons, with polydispersity indices ranging from 1.09 to 1.40 (Fig. 4, inset). It is possible that the poor solubility of the larger dendrimers contributed to less efficient transformations.

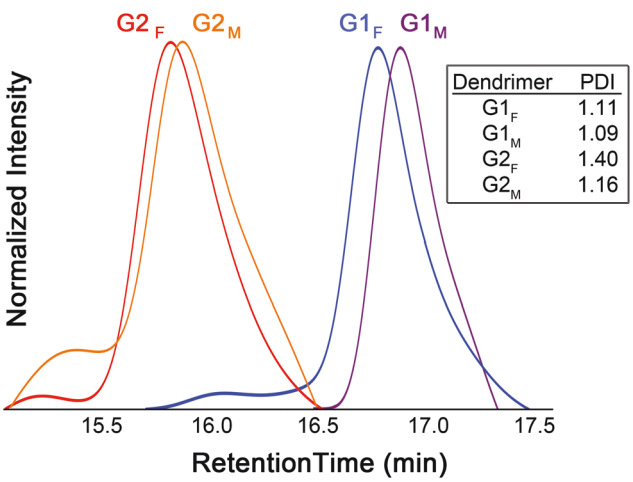

Fig. 4 GPC traces of furan-protected and maleimide-functionalized first and second generation homogeneous dendrimers. Poor solubility prevented GPC analysis of higher generations.

In addition to homogeneous dendrimer **4**, mixed dendrimer **5** was synthesized as an initial example of a "random" dendrimer. As represented schematically in Scheme 2, dendrimer **5** was prepared by thiol-maleimide click addition of 12 equivalents of hydrophilic branched monomer **2** to the $G2_M$ dendrimer. ^{1}H NMR spectroscopy again shows full consumption of the maleimide signal at 6.7 ppm (Fig. S61†). The tetraethylene glycol-functionalized branched monomer **2** was designed and synthesized in hopes that the longer, hydrophilic linkers would increase the overall solubility of resulting dendrimers. Unfortunately, this was not found to be the case as dendrimers above generation 2 were again not sufficiently soluble in common organic solvents (*e.g.* THF, DMF, DMSO, *etc.*) to enable full GPC analysis and prevented further synthesis of higher generation dendrimers. Despite poor solubility, however, the current design still enables a valuable proof-of-concept of the utility of the orthogonal thiol-maleimide/furan-maleimide design.

Conclusions

The combination of thiol-maleimide click chemistry with dynamic covalent furan-maleimide cycloaddition reactions can provide a convenient means of synthesizing dendrimers. The orthogonality of these two maleimide chemistries enables facile and selective addition of thiols to unprotected maleimide derivatives, leaving the alkene of furan-protected maleimide groups untouched. Growing dendrimers can then be activated simply by a thermal retro-Diels–Alder reaction, with the only byproduct being thermally labile furan. Both reactions typically proceed in high yields, are atom economical, and can be easily monitored using diagnostic singlets in their ^{1}H NMR spectra. The dendrons and dendrimers reported herein demonstrate this proof-of-concept, however the current branched monomer designs have their drawbacks. Most notably, the synthesis of branched monomers **1** and **2** require multiple steps and the poor solubility of dendrons and dendrimers synthesized using branched monomers **1** and/or **2** limits their growth. Current work is focused on the synthesis of a more diverse set of additional branched monomers that share the same fundamental design incorporating a focal thiol and furan-protected maleimide branches but can be prepared more efficiently and lead to more soluble dendrimer products. Even a small number of branched monomers incorporating these design features can provide the inputs for a wide variety of homogeneous, sequential, multi-layered, and random dendrimers given that the orthogonality of the thiol-maleimide/furan-maleimide approach allows any such branched monomer to be incorporated into the dendrimer structure at any growth step. Research aimed at expanding the proof-of-concept reported herein is underway.

Conflicts of interest

There are no conflicts to declare.

Acknowledgements

The authors gratefully acknowledge financial support from the National Science Foundation CAREER program (award CHE-1352239) and from Wesleyan University.

Notes and references

1 D. A. Tomalia, H. Baker, J. Dewald, M. Hall, G. Kallos, S. Martin, J. Roech, J. Ryder and P. Smith, *Polym. J.*, 1985, **17**, 117.
2 G. R. Newkome, Z. Yao, G. R. Baker and V. K. Gupta, *J. Org. Chem.*, 1985, **50**, 2003.
3 C. J. Hawker and J. M. J. Fréchet, *J. Am. Chem. Soc.*, 1990, **112**, 7638.
4 B. Helms and E. W. Meijer, *Science*, 2006, **313**, 929.
5 D. Wang, C. Deraedt, J. Ruiz and D. Astruc, *Acc. Chem. Res.*, 2015, **48**, 1871.
6 F. Giacalone, V. Campisciano, C. Calabrese, V. La Parola, Z. Syrgiannis, M. Prato and M. Gruttadauria, *ACS Nano*, 2016, **10**, 4627.
7 A.-M. Caminade, A. Ouali, R. Laurent, C.-O. Turrin and J.-P. Majoral, *Coord. Chem. Rev.*, 2016, **308**, 478.
8 R. M. Kannan, E. Nance, S. Kannan and D. A. Tomalia, *J. Intern. Med.*, 2014, **276**, 579.
9 P. Kesharwani and A. K. Lyer, *Drug Discovery Today*, 2015, **20**, 536.
10 L.-P. Wu, M. Ficker, J. B. Christensen, P. N. Trohopoulos and S. M. Moghimi, *Bioconjugate Chem.*, 2015, **26**, 1198.
11 M. Kawa and J. M. J. Fréchet, *Chem. Mater.*, 1998, **10**, 286.
12 F. Vögtle, S. Gestermann, R. Hesse, H. Schwierz and B. Windisch, *Prog. Polym. Sci.*, 2000, **25**, 987.
13 H.-J. Sun, S. Zhang and V. Percec, *Chem. Soc. Rev.*, 2015, **44**, 3900.
14 H. Ma, F. Li, P. Li, H. Wang, M. Zhang, G. Zhang, M. Baumgarten and K. Müllen, *Adv. Funct. Mater.*, 2016, **26**, 2025.
15 H. C. Klob, M. G. Finn and K. B. Sharpless, *Angew. Chem., Int. Ed.*, 2001, **40**, 2004.
16 C. W. Tornøe, C. Christensen and M. Meldal, *J. Org. Chem.*, 2002, **67**, 3057.
17 W. Xi, T. F. Scott, C. J. Kloxin and C. N. Bowman, *Adv. Funct. Mater.*, 2014, **24**, 2572.
18 P. Espeel and F. E. Du Prez, *Macromolecules*, 2010, **48**, 2.
19 M. Arseneault, C. Wafer and J.-F. Morin, *Molecules*, 2015, **20**, 9263.
20 P. Antoni, D. Nyström, C. J. Hawker, A. Hult and M. Malkoch, *Chem. Commun.*, 2007, 2249.
21 K. L. Killops, L. M. Campos and C. J. Hawker, *J. Am. Chem. Soc.*, 2008, **130**, 5062.
22 X. Ma, J. Tang, Y. Shen, M. Fan, H. Tang and M. Radosz, *J. Am. Chem. Soc.*, 2009, **131**, 14795.
23 M. I. Montañez, L. M. Campos, P. Antoni, Y. Hed, M. V. Walter, B. Krull, A. Khan, A. Hult, C. J. Hawker and M. Malkoch, *Macromolecules*, 2010, **43**, 6004.

24 P. Antoni, M. J. Robb, L. Campos, M. Montañez, A. Hult, E. Malström, M. Malkoch and C. J. Hawker, *Macromolecules*, 2010, **43**, 6625.
25 Y. Sen, Y. Ma and Z. Li, *J. Polym. Sci., Part A: Polym. Chem.*, 2013, **51**, 708.
26 A. Chatani, M. Podgórski, C. Wang and C. N. Bowman, *Macromolecules*, 2014, **47**, 4894.
27 N. Kottari, Y. M. Chabre, T. C. Shiao, R. Rej and R. Roy, *Chem. Commun.*, 2014, **50**, 1983.
28 R. Sharma, K. Naresh, Y. M. Chabre, R. Rej, N. K. Saadeh and R. Roy, *Polym. Chem.*, 2014, **5**, 4321.
29 Z. Zhang, S. Fend and J. Zhang, *Macromol. Rapid Commun.*, 2016, **37**, 318.
30 R. S. Bagul, M. Hosseini, T. C. Shiao, N. K. Saadeh and R. Roy, *Polym. Chem.*, 2017, **8**, 5354.
31 B. H. Northrop, S. H. Frayne and U. Choudhary, *Polym. Chem.*, 2015, **6**, 3415.
32 R. C. Boutelle and B. H. Northrop, *J. Org. Chem.*, 2011, **76**, 7994.
33 O. K. Farha, R. L. Julius and M. F. Hawthorne, *Tetrahedron Lett.*, 2006, **47**, 2619.
34 R. M. Stolz and B. H. Northrop, *J. Org. Chem.*, 2013, **78**, 8105.
35 The retro-Diels–Alder reaction can also be carried out at 100 °C for 12–18 h, which can be beneficial for compounds that are not as thermally stable as those reported herein. Furan deprotection temperatures can be decreased even further if carried out under reduced pressure, which disrupts the dynamic covalent nature of the furan-maleimide reaction by removing furan from the equilibrium.